Int J Clin Exp Pathol 2020;13(5):1159-1168
www.ijcep.com /ISSN:1936-2625/IJCEP0108668

Original Article

Diagnostic performances of the KWAK-TIRADS classification, elasticity score, and Bethesda System for Reporting Thyroid Cytopathology of TI-RADS category 4 thyroid nodules

Supeng Huang[1*], Ning Meng[1*], Mengting Pan[2], Bo Yu[2], Juan Liu[3], Kailin Deng[3], Mingrong Hu[1], Hongwei Zhou[1], Chao Qin[1]

Departments of [1]Thyroid and Breast Surgery, [2]Ultrasound, [3]Pathology, The Affiliated Hospital of Hangzhou Normal University, Hangzhou, China. [*]Equal contributors.

Received February 3, 2020; Accepted April 13, 2020; Epub May 1, 2020; Published May 15, 2020

Abstract: Objective: To explore the value of the KWAK Thyroid Imaging Reporting and Data System (KWAK-TIRADS), elasticity score (ES), and Bethesda System for Reporting Thyroid Cytopathology (BSRTC) in the diagnosis of suspicious thyroid nodules. Materials and methods: The study included 392 cases of TI-RADS category 4 thyroid nodules that underwent thyroidectomy between January 2017 and October 2019. All patients underwent ultrasonography, ultrasound elastography, and fine-needle aspiration cytology (FNAC) before surgery. The nodules were classified into different categories based on the KWAK-TIRADS, ES, and BSRTC. Patients were divided into two groups based on postoperative pathological characteristics. The sensitivity (Se), specificity (Sp), and area under the receiver operating characteristic (ROC) curve were calculated. Student's t-test and Pearson chi-square test were used to compare diagnostic performance. Results: There were 159 patients in the benign group and 233 in the malignant group. The percentage of malignant nodules in KWAK-TIRADS categories 4a, 4b, and 4c were 44.3%, 64.8%, and 92.9%, respectively. The percentages of malignant nodules in ES 2, 3, 4, and 5 were 0%, 37.1%, 93.8%, and 100%, respectively. The percentage of malignant nodules in BSRTC levels I, II, III, IV, V and VI were 57.1%, 2.8%, 9.9%, 76.6%, 99.1%, and 100%, respectively. Among those methods, the BSRTC had better diagnostic efficiency than the KWAK-TIRADS and ES (Sp 81.1%, Se 93.6%, and AUC 0.918, $P<0.01$). Among the combined methods, KWAK-TIRADS+ES+BSRTC was more effective than KWAK-TIRADS+ES, KWAK-TIRADS+BSRTC, and ES+BSRTC (Sp 93.7%, Se 91.4%, and AUC 0.967, $P<0.01$). Conclusion: The combination of KWAK-TIRADS, ES, and BSRTC can improve the accuracy of identifying category 4 thyroid nodules.

Keywords: KWAK-TIRADS, ultrasonic elastography, Bethesda System for Reporting Thyroid Cytopathology, thyroid nodule, diagnosis

Introduction

Thyroid nodules are a common clinical problem with a prevalence of 19% to 68% in the general population [1, 2], and approximately 7% to 15% of thyroid nodules are cancerous, accounting for 96% of all new endocrine cancers [3, 4]. The 5-year survival rate of tumors restricted to the thyroid can reach 99.8%, while that of tumors with distant metastasis is only 57.3% [5], suggesting that a good prognosis of thyroid tumors depends on early diagnosis and treatment. Currently, conventional thyroid ultrasonography is widely used in the screening and differential diagnosis of thyroid nodules due to its noninvasiveness, affordability, convenience and reproducibility [6, 7]. To standardize the classification of thyroid nodules, Horvath [8] first proposed the Thyroid Imaging Reporting and Data System (TI-RADS) based on multiple ultrasonic features in 2009. To date, many guidelines have been established for interpreting thyroid ultrasound images [9]. However, the features of atypical thyroid nodules may overlap on conventional ultrasonography, especially for those of TI-RADS category 4 [10, 11], making it diffi-

cult to accurately discriminate benign and malignant lesions. Therefore, improving the accuracy of preoperative diagnosis has become the primary task of clinicians.

The stiffness of tissue indicates the pathology of nodules to some extent [12]. Clinically, the surgeon usually makes a preliminary assessment of the lump after physical examination, and the stiffness of the tumor will be roughly classified as soft, medium, or hard. However, palpation results are susceptible to differences in nodule size, location, and examiner experience [13]. In recent years, ultrasound elastography has been widely used to measure the stiffness of solid tumors and to distinguish between benign and malignant lesions [14]. It is based on a phenomenon wherein soft tissues are more likely to deform after being compressed, and such deformations can be shown in images through color coding, which are used to reflect nodule stiffness information [15]. At present, this technology has been generally applied in liver, breast, prostate and other tumor explorations. In addition, studies have reported that ultrasound elastography complements conventional thyroid ultrasonography through diagnostic stiffness information that increases the specificity and positive predictive value of the technique [16-20]. However, because of the ambiguity associated with the examiner's subjectivity and the characteristics of the nodules, ultrasound elastography has some limitations in the diagnosis of atypical thyroid nodules.

Although noninvasive examination can differentiate the vast majority of thyroid nodules, it has limitations in detecting thyroid microcarcinoma or ultrasound indeterminate nodules. For such suspected nodules, fine-needle aspiration cytology (FNAC) can usually determine their pathologic malignant characteristics at an early stage, which will facilitate early treatment. To address terminology and other issues related to thyroid FNAC, the National Cancer Institute proposed the Bethesda System for Reporting Thyroid Cytopathology (BSRTC) in 2007 [21], which has a high positive predictive value (97%-99%) for malignant FNAC interpretation. Nonetheless, a clear pathologic diagnosis may be impossible in nearly 15% of biopsied nodules due to insufficient material. The combination of noninvasive and invasive examinations may be beneficial for surgeons to make accurate diagnoses for suspected nodules.

In this study, we analyzed the ultrasound and puncture results of 392 TI-RADS category 4 thyroid nodules and sought a better diagnostic method for screening suspected malignant lesions requiring puncture, thereby improving the accuracy of preoperative diagnosis and better guiding clinical treatment.

Materials and methods

Subjects

Patients with thyroid nodules treated surgically in our hospital from January 2017 to October 2019 were included. In this initial cohort, only patients meeting the following criteria were included: 1. Thyroid nodules with 1~4 of the following five suspicious ultrasonic features - "solid nodules, hypoechoic or extremely hypoechoic, irregular boundary, microcalcification, taller-than-wide shape" - based on the classification standard of TI-RADS proposed by Kwak et al [22]; 2. Conventional thyroid ultrasonography, ultrasound elastography and FNAC performed before surgery; and 3. Cytologic results as well as a final diagnosis of the nodules based on postoperative pathology. The exclusion criteria were as follows: 1. Surgery for hyperthyroidism; 2. Previous history of neck radiation or surgery; and 3. Thyroid nodules that do not meet the standard of KWAK-TIRADS. Thyroid nodules were divided into two groups according to the final pathology. Finally, 346 patients (392 nodules) were included, 159 in the benign group and 233 in the malignant group. There were 54 males and 105 females in the benign group, who were aged 38 to 77 years with an average of 51.2±14.7 years. There were 58 males and 175 females in the malignant group, who were aged 24 to 73 years with an average age of 41.6±18.3 years.

All patients were informed of the purpose and significance of the scientific research project and signed informed consent forms. The study was approved by the Ethics Committee of the Affiliated Hospital of Hangzhou Normal University.

Table 1. Scoring methods for different tests

Method of checking	Inspection results	Score
KWAK-TIRADS classification	4a	1
	4b	2
	4c	3
Elastography score (ES)	1	1
	2	2
	3	3
	4	4
	5	5
Bethesda System For Reporting Thyroid Cytopathology (BSRTC)	I	1
	II	2
	III	3
	IV	4
	V	5
	VI	6

Instruments

Philips EPIQ 5 (Holland), Philips IU 22 Colour Doppler Ultrasound System (Holland) and GE LOGIQ 7 or 9 (America) devices were used for ultrasonic examination. A Japanese octagonal cell puncture needle with a diameter of 18 G and a length of 5 cm was used for FNAC.

Methods

Conventional thyroid ultrasonography was performed by two excellent ultrasonologists. They classified the thyroid nodules according to the KWAK-TIRADS classification and elasticity score [13] and were blinded to any other information about the patient. If there was any inconsistency in the results, a second review was conducted, and consensus was reached through discussion. According to the KWAK-TIRADS classification, the nodules were classified as TI-RADS category 4a (one suspicious ultrasonic feature), 4b (two suspicious ultrasonic features), and 4c (three or four suspicious ultrasonic features). TR4b or 4c nodules were diagnosed as malignant lesions, and TR4a nodules were benign. The elasticity score [13] is based on the color-type of the real-time elastography of the tissue, used to determine the softness of the lesion. In our device, green represents tissue of average hardness, red is harder than the average hardness, and blue is softer than the average hardness. The judgment criteria were as follows: 1. The lesion was green overall; 2. The lesion had a mosaic pattern of green and red; 3. The center of the lesion was red, and the rest of the lesion was green; 4. The lesion was red overall; and 5. The lesion and surrounding tissue were red. ES 4 or 5 nodules were diagnosed as malignant lesions, and nodules of ES 3 or less were benign.

FNAC was performed by an experienced surgeon, and the pathologic smear was classified by two outstanding pathologists. According to the BSRTC, the puncture results are divided into 6 levels: I. nondiagnostic or unsatisfactory; II. benign; III. atypia of undetermined significance or follicular lesion of undetermined significance; IV. follicular neoplasm or suspicious for follicular neoplasm; V. suspicious for malignancy; VI. malignant. BSRTC IV or V nodules were diagnosed as malignant lesions, and nodules of level III or less were benign. If there was any inconsistency, a second review was conducted, and consensus was reached through discussion.

The KWAK-TIRADS, ES and BSRTC scores are shown in **Table 1**. Scores were assigned for each nodule, and the total score was calculated. The highest score was 14, and the lowest score was 3. Based on the pathologic results, the specificity and sensitivity of the individual scoring methods and combinations of scoring methods in the diagnosis were calculated.

Statistical analysis

Statistical data were analyzed using SPSS 22.0 statistical analysis software, and the measurement data are expressed as the mean. The differences in the basic characteristics of the benign and malignant lesions were analyzed by the chi-square test or Fisher's exact probability method. The diagnostic effects of KWAK-TIRADS, ES, BSRTC, and the combinations KWAK-TIRADS+ES, KWAK-TIRADS+BSRTC, ES+BSRTC and KWAK-TIRADS+ES+BSRTC were compared using the McNemar chi-square test. Receiver operating characteristic (ROC) curves

Table 2. Various diagnostic methods and pathologic diagnosis of benign and malignant thyroid nodules

Category	Pathologic diagnosis		Malignancy rate (%)	*P*-value
	Benign (n)	Malignant (n)		
KWAK-TIRADS				<0.01
4a	122	97	44.3	
4b	31	57	64.8	
4c	6	79	92.9	
ES				<0.01
2	25	0	0.0	
3	127	75	37.1	
4	7	106	93.8	
5	0	52	100	
BSRTC				<0.01
Level I	3	4	57.1	
Level II	35	1	2.8	
Level III	91	10	9.9	
Level IV	29	95	76.6	
Level V	1	108	99.1	
Level VI	0	15	100	

The difference between benign lesion group and malignant lesion group was statistically significant ($P<0.05$). Abbreviations: TI-RADS = Thyroid Imaging Reporting and Data System; ES = Elasticity score; BSRTC = Bethesda System for Reporting Thyroid Cytopathology.

were constructed, and the areas under the curve (AUCs) were calculated. The 95% confidence interval of the area under the curve was evaluated. The sensitivity and specificity were calculated by comparison with pathologic results. $P<0.05$ was considered significant.

Results

Comprehensive research data

In the malignant group, the KWAK-TIRADS classification identified 97 cases of TR4a, 57 cases of TR4b, and 79 cases of TR4c; in the benign group, the classification identified 122 cases of TR4a, 31 cases of TR4b, and 6 cases of TR4c (**Table 2**; **Figures 1A**, **2A**). The ES identified 75 cases of score 3, 106 cases of score 4, and 52 cases of score 5 in the malignant group and 25 cases of score 2, 127 cases of score 3, and 7 cases of score 4 in the benign group (**Table 2**; **Figures 1B**, **2B**). The BSRTC identified 4 cases of level I, 1 case of level II, 10 cases of level III, 95 cases of level IV, 108 cases of level V, and 15 cases of VI in the malignant group and 3 cases of level I, 35 cases of level II, 91 cases of level III, 29 cases of level IV, and 1 case of level V in the benign group (**Table 2**; **Figures 1C**, **2C**).

Postoperative pathologic results: A total of 392 cases of TI-RADS category 4 thyroid nodules were included in the study. Of the 233 cases in the malignant group, the vast majority were papillary thyroid carcinoma, accounting for 85.4% (199/233), and the rest were follicular thyroid carcinoma, medullary carcinoma, and undifferentiated carcinoma. Of the 159 cases in the benign group, the vast majority were nodular goiter, accounting for 59.1% (94/159), and the rest were thyroid adenoma, Hashimoto's thyroiditis and nodular goiter cystic lesions (**Table 2**; **Figures 1D**, **2D**).

Comparison of the diagnostic efficiency of the KWAK-TIRADS, ES, and BSRTC

The percentage of malignant nodules from the KWAK-TIRADS classification in categories TR4a, 4b, and 4c in this study were 44.3%, 64.8%, and 92.9%, respectively, and the differences were statistically significant ($P<0.01$). The ROC curves demonstrated that the best cut-off point for the KWAK-TIRADS was TR4b. The sensitivity, specificity, and AUC were 75.5%, 76.7%, and 0.787 (95% CI: 0.741-0.832), respectively. The percentage of malignant nodules in groups ES 2, 3, 4, and 5 in this study were 0%, 37.1%, 93.8%, and 100%, respectively, and the differences were statistically significant ($P<0.01$). The ROC curves demonstrated that the best cut-off point for ES was 4. The sensitivity, specificity, and AUC were 67.8%, 95.6%, and 0.847 (95% CI: 0.81-0.885), respectively. The percentage of malignant nodules from the BSRTC in levels I, II, III, IV, V, VI nodules in this study were 57.1%, 2.8%, 9.9%, 76.6%, 99.1%, and 100%, respectively, and the differences were statistically significant ($P<0.01$). The ROC curves demonstrated that the best cut-off point for BSRTC was IV. The sensitivity, specificity, and AUC were 93.6%, 81.1%, and 0.918 (95% CI: 0.889-0.946), respectively.

The results showed that the efficacy of the BSRTC (AUC = 0.918) was larger than that of

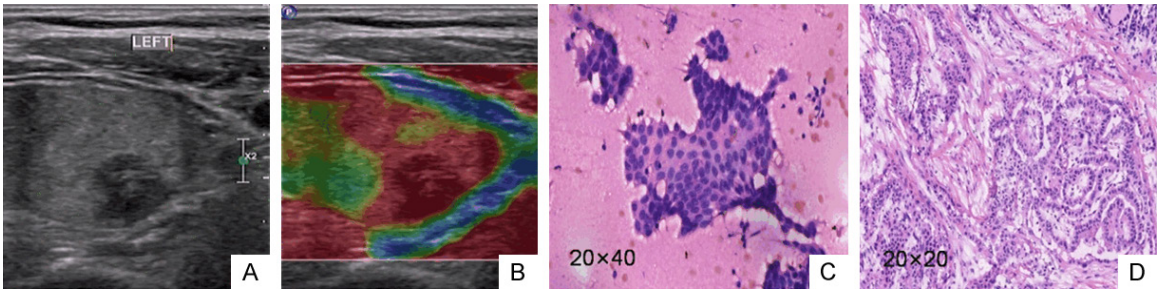

Figure 1. Papillary thyroid carcinoma with elasticity score of 5 and BSRTC of VI in a 55-year-old woman. US images were obtained in transverse plane. A. On conventional US imaging, lesion was classified as KWAK-TIRADS category 4c; B. On elasticity imaging, both the entire hypoechoic lesion and its surrounding area were red; C. Cytologically, the nucleus was significantly enlarged with ground-glass appearance, and a nuclear sulcus was seen (Hematoxylin-eosin stain; 20×40); D. Histologically, the tumor cells were arranged in a papillary shape, the nuclei were crowded, nuclear grooves and nuclear inclusions were visible, and the surrounding thyroid showed Hashimoto's disease. Findings were consistent with papillary thyroid carcinoma (classic) (Hematoxylin-eosin stain; 20×20).

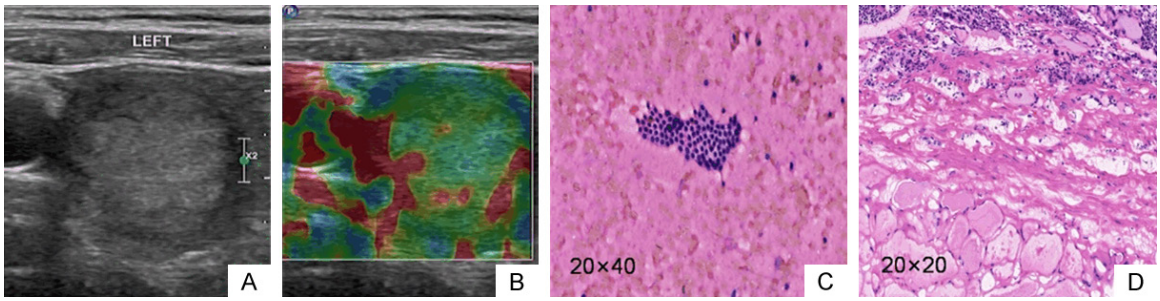

Figure 2. Benign lesions with elasticity score of 2 and BSRTC of II in a 39-year-old woman. US images were obtained in the transverse plane. A. On conventional US imaging, lesion was classified as KWAK-TIRADS category 4a; B. On elasticity imaging, hypoechoic lesion shows a mosaic pattern of green and red; C. Cytologically (benign), the nucleus is small and no changes in nuclear grooves are seen (Hematoxylin-eosin stain; 20×40); D. Histologically, the background is Hashimoto's disease with fibrosis and nodule formation (Hematoxylin-eosin stain; 20×20).

Table 3. Comparison of the various diagnostic methods and combined scoring method in terms of diagnostic efficiency

Method of checking	Cut-off point	Spe (%)	Sens (%)	*P* Value
KWAK-TIRADS	≥2	76.7	75.5	<0.01
ES	≥4	95.6	67.8	<0.01
BSRTC	≥4	81.1	93.6	<0.01
ES+BSRTC	≥7	80.5	96.6	<0.01
KWAK-TIRADS+BSRTC	≥5	94.3	87.6	<0.01
KWAK-TIRADS+ES	≥5	91.8	75.1	<0.01
KWAK-TIRADS+ES+BSRTC	≥8	93.7	91.4	<0.01

McNemar's chi-square test: the difference between benign lesion group and malignant lesion group was statistically significant ($P<0.05$). Abbreviations: TI-RADS = Thyroid Imaging Reporting and Data System; ES = Elasticity score; BSRTC = Bethesda System for Reporting Thyroid Cytopathology.

the ES (AUC = 0.847) and the KWAK-TIRADS (AUC = 0.787) (**Table 4**). BSRTC has higher sensitivity for suspicious nodules, ES has higher specificity, and the differences are all statistically significant ($P<0.01$) (**Figure 3**).

Comparison of the diagnostic efficacy of the combined scoring methods

The results showed that the efficacy of the ES+BSRTC combination (AUC = 0.952) was higher than that of the KWAK-TIRADS+ES combination (AUC = 0.913) and the KWAK-TIRADS+BSRTC combination (AUC = 0.948) but lower than that of the KWAK-TIRADS+ES+BSRTC combination (AUC = 0.967) (**Table 4**; **Figure 4**). The ROC curves showed that the optimal cut-off point of the KWAK-TIRADS+ES+BSRTC combination was 8, that of the ES+BSRTC combination was 7, that of the KWAK-TIRADS+ES combination was 5, and that of the KWAK-TIR-ADS+BSRTC combination was 5. In addition, the sensitivity of the

Table 4. Comparison of ROC curves among various diagnostic methods and combined scoring method

Test result variable(s)	Area	Std. error[a]	Asymptotic sig.[b]	Asymptotic 95% confidence interval	
				Lower bound	Upper bound
KWAK-TIRADS	0.787	0.023	0.00	0.741	0.832
ES	0.847	0.019	0.00	0.810	0.885
BSRTC	0.918	0.014	0.00	0.889	0.946
ES+BSRTC	0.952	0.010	0.00	0.933	0.972
KWAK-TIRADS+BSRTC	0.948	0.012	0.00	0.924	0.972
KWAK-TIRADS+ES	0.913	0.014	0.00	0.886	0.940
KWAK-TIRADS+ES+BSRTC	0.967	0.008	0.00	0.952	0.983

The Receiver operating characteristic (ROC) curves were constructed, and the areas under curve (AUCs) were calculated. [a]Under the nonparametric assumption. [b]Null hypothesis: true area = 0.5. $P<0.05$ was considered statistically significant. Abbreviations: TI-RADS = Thyroid Imaging Reporting and Data System; ES = Elasticity score; BSRTC = Bethesda System for Reporting Thyroid Cytopathology.

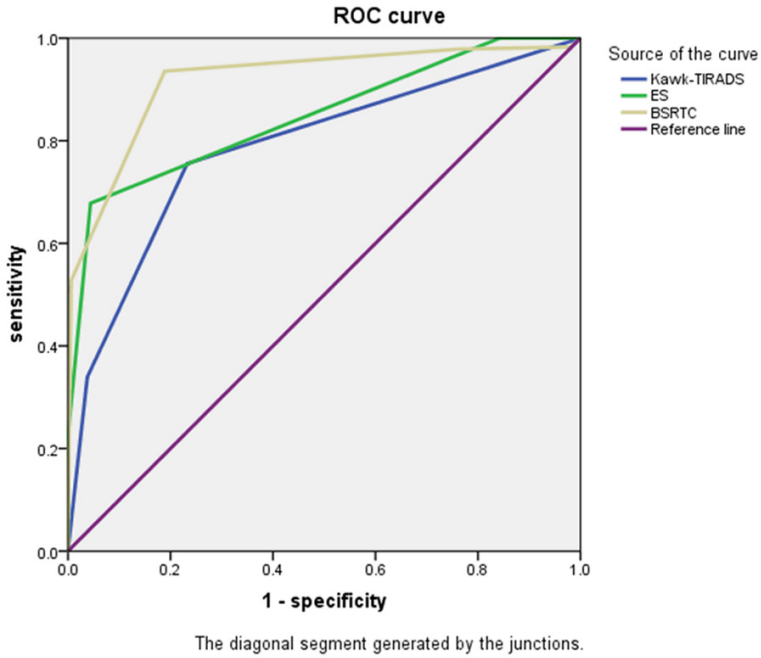

Figure 3. Receiver operating characteristic (ROC) curve of various diagnostic methods. The sensitivity and specificity in the prediction of malignant thyroid nodules. Abbreviations: TI-RADS = Thyroid Imaging Reporting and Data System; ES = Elasticity score; BSRTC = Bethesda System for Reporting Thyroid Cytopathology.

ES+BSRTC combination was higher than that of the other methods, and the sensitivity and specificity of the KWAK-TIRADS+ES+BSRTC combination were quite high; the differences were all statistically significant ($P<0.01$) (**Table 3**).

Discussion

According to the statistics of the National Cancer Institute, the incidence of thyroid cancer in the United States was nearly 54,000 in 2018, accounting for 3.1% of all new malignancies [32]. Furthermore, some research has predicted that thyroid cancer will become the fourth most common cancer by 2030 in the United States [23]. A good prognosis of thyroid tumors can be achieved through early diagnosis and treatment. Conventional thyroid ultrasonography is widely used for the early screening of thyroid cancer because of its noninvasiveness and simplicity. The TI-RADS classification, which is related to conventional ultrasonography, provides a standardization of the imaging features of thyroid nodules. However, the TI-RADS classification has limitations in the differential diagnosis of atypical thyroid nodules, especially those of TI-RADS category 4, which have a risk of malignancy of 5% to 80% [8]. Thus, accurately differentiating benign and malignant thyroid tumors with existing technology remains a major challenge for surgeons [24, 25].

The KWAK-TIRADS classification uses five ultrasound malignant features to assess the risk of malignancy in thyroid nodules. Gao [1] reported that the percentage of malignancy

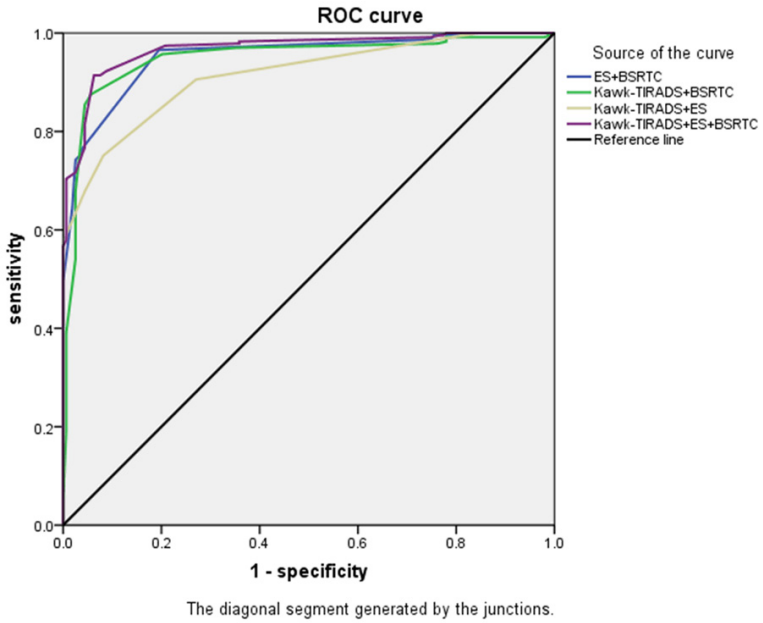

Figure 4. Receiver operating characteristic (ROC) curve of various diagnostic methods. The sensitivity and specificity in the prediction of malignant thyroid nodules. Abbreviations: TI-RADS = Thyroid Imaging Reporting and Data System; ES = Elasticity score; BSRTC = Bethesda System for Reporting Thyroid Cytopathology.

in nodules of categories TR4a, 4b, and 4c were 10.9%, 55.2%, and 88.8%, respectively, which are comparable to those reported in previous studies [26, 27]. In our study, the percentage of malignancy in KWAK-TIRADS category 4a, 4b, and 4c nodules were 44.3%, 64.8%, and 92.9%, respectively. The reason for the result may be that most of the nodules selected in the previous studies were TI-RADS category 2 or 3, while our study contained more cases suspicious for malignancy. Moreover, the sensitivity, specificity and AUC of the KWAK-TIRADS in our study were 75.5%, 76.7% and 0.787, respectively. This shows that the KWAK-TIRADS classification plays a reliable role in the risk stratification of TI-RADS category 4 thyroid nodules. However, the sensitivity is rather low. The reason may be that the ultrasound features of some benign and malignant lesions may overlap, and subjective factors cannot be completely excluded. Therefore, additional tests are needed to improve the diagnostic efficiency of the KWAK-TIRADS.

Ultrasound elastography, which can be used to obtain stiffness information from tissues, is widely used in the diagnosis of thyroid nodules. Itoh [13] reported that the sensitivity and specificity of the ES for 111 cases of thyroid nodules were 89.3% and 93.1%, respectively. Some studies have also shown that the ES has high diagnostic value for thyroid nodules [28, 29]. Our results indicate that the specificity of the ES for TI-RADS category 4 thyroid nodules (95.6%) was comparable to that from the above studies, but the sensitivity was quite low (67.8%). The reasons for these results may be as follows: 1. The small malignant component was not enough to change the overall stiffness, resulting in lower scores; 2. The presence of coarse calcification affected the stiffness of the nodules to a certain extent, resulting in higher scores. For these nodules, it is necessary to combine other examinations to reduce the number of missed diagnoses. In addition, our study suggests that ES is more valuable than the KWAK-TIRADS for the diagnosis of malignant tumors (AUC = 0.847) but less valuable than the KWAK-TIRADS+ES combination (AUC = 0.913). This shows that ultrasound elastography is very valuable for screening suspected malignant nodules, and in combination with KWAK-TIRADS can significantly improve the diagnostic accuracy for suspected malignant nodules.

However, no examination can replace pathologic diagnosis. FNAC usually detects the malignant pathological characteristics of thyroid nodules at an early stage with a high specificity of 60% to 98% [30]. The BSRTC is the standard reporting system for puncture results, which avoids unnecessary surgery for patients with benign nodules and selects the appropriate surgical procedure for patients with thyroid cancer. Studies have shown that most nodules are classified as benign or malignant by BSRTC, but nearly 20% of the biopsied nodules still retain an “indeterminate” cytology [31]. Our data showed that among the three methods, the BSRTC had the highest diagnostic value for malignant tumors (AUC =

0.916) and that the diagnostic value of the BSRTC+ES combination was higher than the value of the BSRTC and the BSRTC+KWAK-TIRADS combination (AUC = 0.952) but below the diagnostic value of the BSRTC+KWAK-TIRADS+ES combination (AUC = 0.967). The ROC curve of the three joint scoring methods had the largest area, indicating that its diagnostic value is large and deserves further investigation. These results show that combining the KWAK-TIRADS, ES, and BSRTC can effectively improve the diagnostic accuracy of TI-RADS category 4 thyroid nodules. Therefore, noninvasive examination combined with invasive examination for the management of suspicious malignant nodules can avoid more expensive molecular tests.

There are several limitations in this study. First, this is a single-center study of a small number of samples; the accuracy of preoperative diagnosis could be improved if our results are validated in a larger group of thyroid centers. Second, most of the malignant nodules involved in this study were papillary thyroid carcinomas, and the vast majority of the benign nodules were nodular goiters. The diagnostic value of this method for other benign and malignant thyroid pathologic types undoubtedly requires further investigation with a larger sample size and a multicenter study. Third, the ultrasound examination and FNAC in this study are highly dependent on the operator's experience and are also affected by the patient's cooperation. Furthermore, the determinations of the KWAK-TIRADS and ES categories were made at the same time, and it is possible that the observers were affected by results with higher classifications.

In conclusion, the KWAK-TIRADS classification combined with the elasticity score can distinguish the majority of nodules, and for nodules that are still difficult to identify, FNAC can be used as an effective supplementary diagnostic measure.

Disclosure of conflict of interest

None.

Address correspondence to: Chao Qin, Department of Thyroid and Breast Surgery, The Affiliated Hospital of Hangzhou Normal University, No. 126, Wenzhou Road, Hangzhou 310015, China. E-mail: qinchao0127@126.com

References

[1] Gao L, Xi X, Jiang Y, Yang X, Wang Y, Zhu S, Lai X, Zhang X, Zhao R and Zhang B. Comparison among TIRADS (ACR TI-RADS and KWAK-TI-RADS) and 2015 ATA guidelines in the diagnostic efficiency of thyroid nodules. Endocrine 2019; 64: 90-96.

[2] Ahmadi S, Oyekunle T, Jiang X, Scheri R, Perkins J, Stang M, Roman S and Sosa JA. A direct comparison of the ATA and TI-RADS ultrasound scoring systems. Endocr Pract 2019; 25: 413-422.

[3] Leenhardt L, Erdogan MF, Hegedus L, Mandel SJ, Paschke R, Rago T and Russ G. 2013 European thyroid association guidelines for cervical ultrasound scan and ultrasound-guided techniques in the postoperative management of patients with thyroid cancer. Eur Thyroid J 2013; 2: 147-159.

[4] Hegedüs L. Clinical practice. The thyroid nodule. N Engl J Med 2004; 351: 1764-1771.

[5] Siegel R, Naishadham D and Jemal A. Cancer statistics, 2012. CA Cancer J Clin 2012; 62: 10-29.

[6] Ha EJ, Baek JH and Na DG. Risk stratification of thyroid nodules on ultrasonography: current status and perspectives. Thyroid 2017; 27: 1463-1468.

[7] Grani G, Lamartina L, Ascoli V, Bosco D, Nardi F, D'Ambrosio F, Rubini A, Giacomelli L, Biffoni M, Filetti S, Durante C and Cantisani V. Ultrasonography scoring systems can rule out malignancy in cytologically indeterminate thyroid nodules. Endocrine 2017; 57: 256-261.

[8] Horvath E, Majlis S, Rossi R, Franco C, Niedmann JP, Castro A and Dominguez M. An ultrasonogram reporting system for thyroid nodules stratifying cancer risk for clinical management. J Clin Endocrinol Metab 2009; 94: 1748-1751.

[9] Giorgio G, Livia L, Vito C, Marianna M, Piernatale L and Cosimo D. Interobserver agreement of various thyroid imaging reporting and data systems. Endocr Connect 2018; 7: 1-7.

[10] Giusti M, Campomenosi C, Gay S, Massa B, Silvestri E, Monti E and Turtulici G. The use of semi-quantitative ultrasound elastosonography in combination with conventional ultrasonography and contrast-enhanced ultrasonography in the assessment of malignancy risk of thyroid nodules with indeterminate cytology. Thyroid Res 2014; 7: 9.

[11] Liu Y, Wu H, Zhou Q, Gou J, Xu J, Liu Y and Chen Q. Diagnostic value of conventional ultrasonography combined with contrast-enhanced ultrasonography in thyroid imaging reporting and data system (TI-RADS) 3 and 4 thyroid micronodules. Med Sci Monit 2016; 22: 3086-3094.

[12] Shin JH, Baek JH, Chung J, Ha EJ, Kim JH, Lee YH, Lim HK, Moon WJ, Na DG, Park JS, Choi YJ, Hahn SY, Jeon SJ, Jung SL, Kim DW, Kim EK, Kwak JY, Lee CY, Lee HJ, Lee JH, Lee JH, Lee KH, Park SW and Sung JY; Korean Society of Thyroid Radiology (KSThR) and Korean Society of Radiology. Ultrasonography diagnosis and imaging-based management of thyroid nodules: revised korean society of thyroid radiology consensus statement and recommendations. Korean J Radiol 2016; 17: 370-395.

[13] Itoh A, Ueno E, Tohno E, Kamma H, Takahashi H, Shiina T, Yamakawa M and Matsumura T. Breast disease: clinical application of US elastography for diagnosis. Radiology 2006; 239: 341-350.

[14] Han RJ, Du J, Li FH, Zong HR, Wang JD, Shen YL and Zhou QY. Comparisons and combined application of two-dimensional and three-dimensional real-time shear wave elastography in diagnosis of thyroid nodules. J Cancer 2019; 10: 1975-1984.

[15] Xie J, Zou L, Yao M, Xu G, Zhao L, Xu H and Wu R. A preliminary investigation of normal pancreas and acute pancreatitis elasticity using virtual touch tissue quantification (VTQ) imaging. Med Sci Monit 2015; 21: 1693-1699.

[16] Samir AE, Dhyani M, Anvari A, Prescott J, Halpern EF, Faquin WC and Stephen A. Shear-wave elastography for the preoperative risk stratification of follicular-patterned lesions of the thyroid: diagnostic accuracy and optimal measurement plane. Radiology 2015; 277: 565-573.

[17] Choi WJ, Park JS, Koo HR, Kim SY, Chung MS and Tae K. Ultrasound elastography using carotid artery pulsation in the differential diagnosis of sonographically indeterminate thyroid nodules. AJR Am J Roentgenol 2015; 204: 396-401.

[18] Rago T, Scutari M, Santini F, Loiacono V, Piaggi P, Di Coscio G, Basolo F, Berti P, Pinchera A and Vitti P. Real-time elastosonography: useful tool for refining the presurgical diagnosis in thyroid nodules with indeterminate or nondiagnostic cytology. J Clin Endocrinol Metab 2010; 95: 5274-5280.

[19] Nell S, Kist JW, Debray TP, de Keizer B, van Oostenbrugge TJ, Borel Rinkes IH, Valk GD and Vriens MR. Qualitative elastography can replace thyroid nodule fine-needle aspiration in patients with soft thyroid nodules. A systematic review and meta-analysis. Eur J Radiol 2015; 84: 652-661.

[20] Cappelli C, Pirola I, Gandossi E, Agosti B, Cimino E, Casella C, Formenti A and Castellano M. Real-time elastography: a useful tool for predicting malignancy in thyroid nodules with non-diagnostic cytologic findings. J Ultrasound Med 2012; 31: 1777-1782.

[21] Cibas ES and Ali SZ. The Bethesda System for Reporting Thyroid Cytopathology. Thyroid 2009; 19: 1159-1165.

[22] Kwak JY, Han KH, Yoon JH, Moon HJ, Son EJ, Park SH, Jung HK, Choi JS, Kim BM and Kim EK. Thyroid imaging reporting and data system for US features of nodules: a step in establishing better stratification of cancer risk. Radiology 2011; 260: 892-899.

[23] Rahib L, Smith BD, Aizenberg R, Rosenzweig AB, Fleshman JM and Matrisian LM. Projecting cancer incidence and deaths to 2030: the unexpected burden of thyroid, liver, and pancreas cancers in the United States. Cancer Res 2014; 74: 2913-2921.

[24] Chng CL, Kurzawinski TR and Beale T. Value of sonographic features in predicting malignancy in thyroid nodules diagnosed as follicular neoplasm on cytology. Clin Endocrinol (Oxf) 2015; 83: 711-716.

[25] Pang T, Huang L, Deng Y, Wang T, Chen S, Gong X and Liu W. Logistic regression analysis of conventional ultrasonography, strain elastosonography, and contrast-enhanced ultrasound characteristics for the differentiation of benign and malignant thyroid nodules. PLoS One 2017; 12: e0188987.

[26] Xu T, Gu JY, Ye XH, Xu SH, Wu Y, Shao XY, Liu DZ, Lu WP, Hua F, Shi BM, Liang J, Xu L, Tang W, Liu C and Wu XH. Thyroid nodule sizes influence the diagnostic performance of TIRADS and ultrasound patterns of 2015 ATA guidelines: a multicenter retrospective study. Sci Rep 2017; 7: 43183.

[27] Cheng SP, Lee JJ, Lin JL, Chuang SM, Chien MN and Liu CL. Characterization of thyroid nodules using the proposed thyroid imaging reporting and data system (TI-RADS). Head Neck 2013; 35: 541-547.

[28] Ragazzoni F, Deandrea M, Mormile A, Ramunni MJ, Garino F, Magliona G, Motta M, Torchio B, Garberoglio R and Limone P. High diagnostic accuracy and interobserver reliability of real-time elastography in the evaluation of thyroid nodules. Ultrasound Med Biol 2012; 38: 1154-1162.

[29] Asteria C, Giovanardi A, Pizzocaro A, Cozzaglio L, Morabito A, Somalvico F and Zoppo A. US-elastography in the differential diagnosis of benign and malignant thyroid nodules. Thyroid 2008; 18: 523-531.

[30] Tee YY, Lowe AJ, Brand CA and Judson RT. Fine-needle aspiration may miss a third of all malignancy in palpable thyroid nodules: a comprehensive literature review. Ann Surg 2007; 246: 714-720.

[31] Jeong SH, Hong HS, Lee EH, Cha JG, Park JS and Kwak JJ. Outcome of thyroid nodules characterized as atypia of undetermined significance or follicular lesion of undetermined significance and correlation with ultrasound features and BRAF(V600E) mutation analysis. AJR Am J Roentgenol 2013; 201: W854-860.

[32] National Cancer Institute. Surveillance, Epidemiology, and End Results Program. Cancer stat facts: thyroid cancer. Source Accessed January 15, 2019.